J. Astrophys. Astr. (1984) 5, 169–180

Effects of Partial Frequency Redistribution Functions R_{II}, R_{III} and R_V on Source Functions

D. Mohan Rao, K. E. Rangarajan & A. Peraiah *Indian Institute of Astrophysics, Bangalore 560034*

Received 1982 May 20; accepted 1984 March 1

Abstract. The effects of partial frequency redistribution on the formation of spectral lines have been studied. We considered the angle-averaged R_{II}, R_{III} and R_V types of redistribution with isotropic phase function. Transfer equation with plane-parallel geometry is solved in isothermal atmospheres. For an atmosphere with constant thermal sources, the frequency-dependent source function $S_L(R_V)$ lies below $S_L(R_{III})$ but above $S_L(R_{II})$ in the line wings.

Key words: radiative transfer—partial frequency redistribution—line source functions—spectral line formation

1. Introduction

Frequency-dependent source functions were studied by Hummer (1969) in semi-infinite and finite isothermal atmospheres. In the wings, large differences were found to exist between the complete redistribution (CRD) and partial redistribution (PRD) source functions. The effects of photon frequency and angular redistribution on line formation using R_I, R_{II} and R_{III} functions and their role in finite and semi-infinite plane-parallel media were studied in a series of papers by Vardavas (1976 a,b,c), using angle-dependent redistribution functions. Vardavas made a comparison with CRD and also with the results of angle-averaged redistribution functions. The differences between the emergent profiles using CRD with a Voigt absorption profile and R_{III} function was found to be negligible (Vardavas 1976 b). Similar conclusion was arrived at by Finn (1967). R_{II} redistribution function, which is strongly coherent in the wings, was shown to lower the line profile outside the Doppler core (Hummer 1969; Vardavas 1976 c). R_I angle-dependent and angle-averaged redistribution functions were studied in spherically symmetric expanding media by Peraiah (1978). In moving media he obtained P-Cygni type of profiles. Milkey & Mihalas (1973) used a combination of R_{II} and R_{III} redistribution functions in explaining Solar Lyman-α resonance-line profile.

As far as subordinate lines are concerned, Heinzel (1981) derived the correct laboratory frame redistribution function (LFR) for the scattering of radiation assuming both the atomic levels to be radiatively broadened. This LFR denoted as $R_V(x', \hat{n}'; x, \hat{n})$ is based on quantum-mechanical results of Omont, Smith & Cooper (1972). R_V can be applied in low-density media like chromospheres, gaseous nebulae *etc.*, where collisions are few. In a subsequent paper, Heinzel & Hubený (1982) extended their LFR to include collisional broadening of both the levels. Some transfer effects of R_V have been discussed by Hubený & Heinzel (1984).

The aim of this paper is to study the influence of angle-averaged R_V redistribution function in radiative transfer calculations. To make a comparative study, we also evaluated the source functions using R_{II} and R_{III}. In Section 2 we have briefly discussed the functions R_{II}, R_{III} and R_V. We have described the basic equations and the computational procedure in Section 3. Results are discussed in Section 4.

2. Redistribution functions

When the lower level is sharp and the upper level is radiatively broadened (assuming isotropic phase function), the redistribution function is given by (Hummer 1962)

$$R_{II}(x', x) = \frac{1}{\pi^{3/2}} \int_{\frac{|x'-x|}{2}}^{\infty} e^{-u^2} \left[\tan^{-1}\left(\frac{\underline{x}+u}{a_j}\right) - \tan^{-1}\left(\frac{\bar{x}-u}{a_j}\right)\right] du, \quad (1)$$

where $\bar{x} = \max(|x|, |x'|)$ and $\underline{x} = \min(|x|, |x'|)$, x' is the frequency of incoming photon measured in Doppler width units, x is the frequency of emitted photon and a_j is the damping constant for the upper level. We chose $a_j = 2 \times 10^{-3}$ and evaluated the above function. The profile function $\phi(x)$ is given by

$$\phi(x) = \int_{-\infty}^{\infty} R_{II}(x', x)\, dx' = H(a_j, x), \quad (2)$$

where $H(a_j, x)$ is the normalized Voigt function. We have plotted $R_{II}(x', x)/\phi(x')$ in Fig. 1(a). This quantity is the probability of emission at frequency x per absorption, when the absorption is at frequency x'. From this figure we see the coherency for wing photons and that they have the least probability of being emitted at the line centre. In the Doppler core, R_{II} behaves like other redistribution functions.

Radiative and collisional broadening of the upper level with isotropic phase function gives rise to a redistribution function of the form

$$R_{III}(x', x) = \frac{1}{\pi^{5/2}} \int_0^{\infty} e^{-u^2} \left[\tan^{-1}\left(\frac{x'+u}{a_j}\right) - \tan^{-1}\left(\frac{x'-u}{a_j}\right)\right] \times \left[\tan^{-1}\left(\frac{x+u}{a_j}\right) - \tan^{-1}\left(\frac{x-u}{a_j}\right)\right] du. \quad (3)$$

The absorption profile function in this case is defined in a similar way as above. We have plotted $R_{III}(x', x)/\phi(x')$ for $a_j = 2 \times 10^{-3}$ and 10^{-3} in Fig. 1(b) and (c) respectively. $R_{II, III}$ are generated using Simpson's rule with small intervals. From these figures we see that the wing photons get completely redistributed and they have a high probability of being emitted at the centre.

When the lower and upper levels are broadened by radiative damping, the angle-dependent LFR is given by (Heinzel 1981)

$$R_V(x', \hat{n}'; x, \hat{n}) = \frac{1}{4\pi^2 \sin\theta} \left[H\left(a_j \sec\frac{\theta}{2}, \frac{x+x'}{2}\sec\frac{\theta}{2}\right) H\left(a_j \csc\frac{\theta}{2}, \frac{x-x'}{2}\csc\frac{\theta}{2}\right) + E_V(x', x, \theta)\right], \quad (4)$$

where θ is the angle between incoming ($\hat{n}'$) and outgoing ($\hat{n}$) photon directions. The

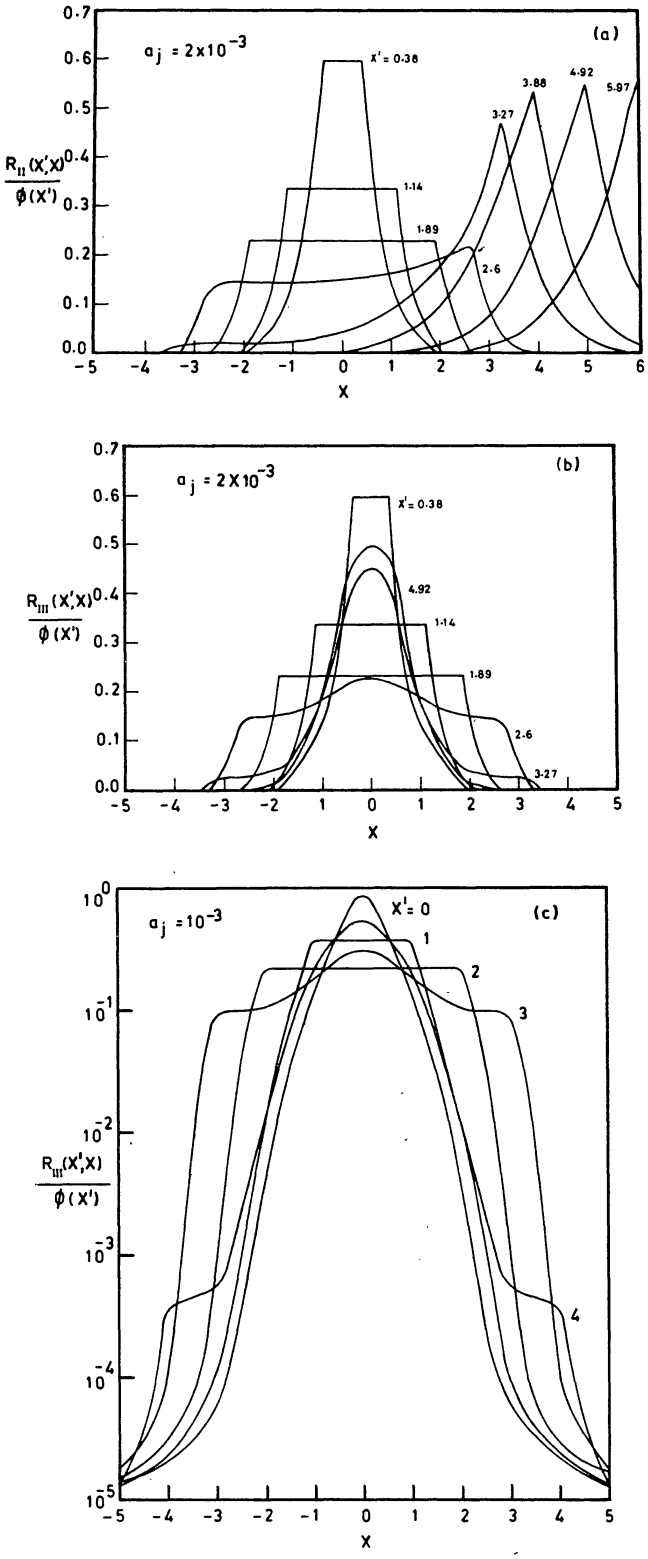

Figure 1. The probability of emission $R(x', x)/\phi(x')$ at frequency x per absorption when the absorption is at frequency x' is plotted for (a) R_{II} with $a_j = 2\times10^{-3}$, (b) R_{III} with $a_j = 2\times10^{-3}$, and (c) R_{III} with $a_j = 10^{-3}$.

function E_V is given by

$$E_V(x', x, \theta) = \frac{\sin(\theta/2)}{\pi^{1/2}} \mathrm{Re} \int_0^\infty e^{-t^2}(e^{-2wt} + e^{-2w't})\Delta(t)dt, \quad (5)$$

where

$$\Delta(t) = D\left(z + t\cos\frac{\theta}{2} + a_i \sec\frac{\theta}{2}\right) - D\left(z + t\cos\frac{\theta}{2}\right),$$

$$z = \sec\frac{\theta}{2}\left(a_j - i\frac{x+x'}{2}\right),$$

$$w = a_i + a_j - ix,$$

$$w' = a_i + a_j - ix',$$

$$D(\omega) = H(p, q) + iK(p, q),$$

$$\omega = p - iq,$$

a_i and a_j being the damping constants for lower and upper levels respectively. The common Voigt functions $H(p, q)$ and $K(p, q)$ were computed using the method due to Matta & Reichel (1971).

The angle-averaged expression can be obtained by

$$R_V(x', x) = 8\pi^2 \int_0^\pi R_V(x', x, \theta)\sin\theta\, d\theta. \quad (6)$$

The corresponding absorption profile is

$$\phi(x) = \int_{-\infty}^{\infty} R_V(x', x)dx = H(a_i + a_j, x). \quad (6a)$$

We have used the method employed by Heinzel (1981) to evaluate $E_V(x', x, \theta)$. We have also included the second-order terms in computing the E-function following Heinzel & Hubený (1983). To evaluate the angle-averaged function R_V, we have adopted the procedure described in detail by Heinzel & Hubený (1983). The atomic frame redistribution (AFR), r_V, has maxima at $\xi = \xi'$ and $\xi = \xi_0$ (ξ', ξ and ξ_0 being the absorption, emission and line-centre frequencies in the atomic frame). The underlying physics is discussed for example by Mihalas (1978). We have plotted $R_V(x', x)/\phi(x')$ in Fig. 2. From this figure we see that a photon, when absorbed in the wings, has a high probability of being emitted in the wing as well as at the centre. The wing emission is like that of R_{II} function and the emission at the centre is like that of R_{III}.

3. Basic equations and the computational procedure

The equation of transfer for a two-level atom with plane-parallel geometry is given by,

$$\mu\frac{d}{dz}I(x, \mu, z) = K_L(z)[\beta + \phi(x)][S(x, z) - I(x, \mu, z)] \quad (7)$$

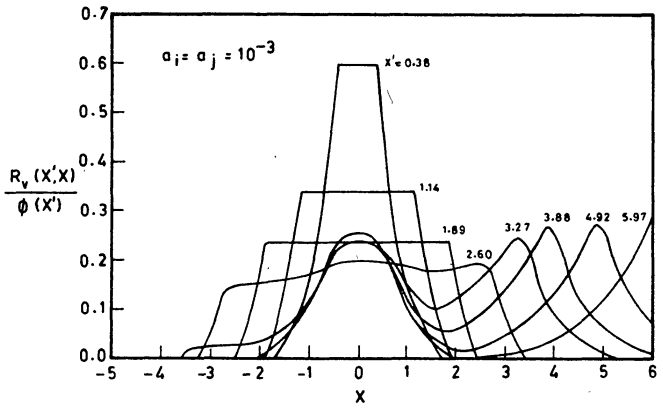

Figure 2. The probability $R_V(x', x)/\phi(x')$ for different x' for $a_i = a_j = 10^{-3}$.

and for the oppositely directed beam

$$-\mu\frac{d}{dz}I(x, -\mu, z) = K_L(z)[\beta+\phi(x)][S(x, z)-I(x, -\mu, z)] \tag{8}$$

where $I(x, \mu, z)$ is the specific intensity at angle $\cos^{-1}\mu$ $[\mu\in(0, 1)]$ at the geometrical point z, and frequency $x = (\nu-\nu_0)/\Delta s$, Δs being some standard frequency interval. The source function $S(x, z)$ is given by

$$S(x, z) = \frac{\phi(x)S_L(x, z)+\beta S_C}{\phi(x)+\beta}, \tag{9}$$

where S_L and S_C refer to the source function in the line and continuum respectively.

The line source function is given by

$$S_L(x, z) = \frac{(1-\varepsilon)}{\phi(x)}\int_{-\infty}^{\infty} R(x', x)\, J(x')\, dx' + \varepsilon B \tag{10}$$

where ε is the probability per scatter that a photon is destroyed by collisional de-excitation. B is the Planck function. We have set $S_C = B = 1$. β is the ratio of continuous opacity per Doppler width to the line opacity.

We have solved the above equations within the framework of discrete-space-theory technique (Grant & Peraiah 1972). The complete procedure with the computer code is given by Peraiah (1978). Gaussian quadrature points were used for frequency and angular mesh. 24 frequency points and two angles were chosen. Since the equations admit a solution which is symmetric with respect to the line centre, we considered only the positive frequency grid. Then for the evaluation of the scattering integral we adopted the technique described by Adams, Hummer & Rybicki (1971).

4. Results and discussion

Fig. 3 gives the emergent intensity as a function of frequency for a purely-scattering

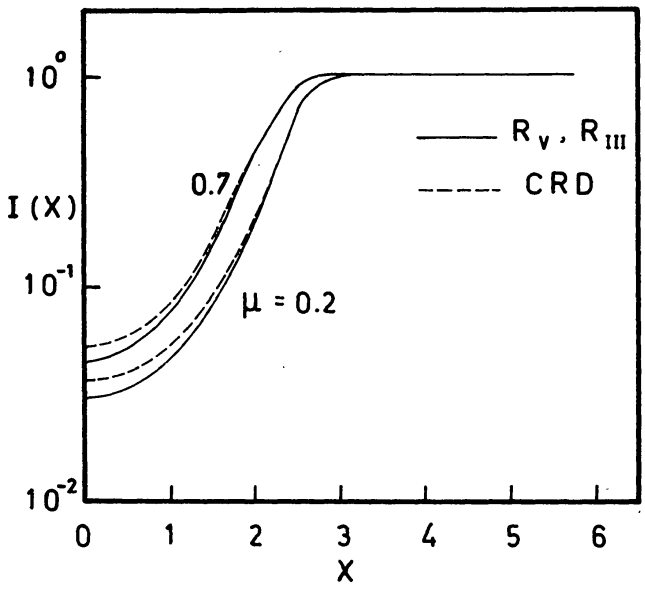

Figure 3. Emergent intensities for R_V and R_{III} are compared with CRD at $\mu = 0.2$ and 0.7 for the case $\varepsilon = \beta = 0$.

atmosphere. The CRD case with Voigt absorption profile and damping parameter $a = 2 \times 10^{-3}$ is also plotted for comparison purposes. Boundary conditions considered are

$$I(x, \mu, \tau = T) = 1; \quad I(x, -\mu, \tau = 0) = 0. \tag{11}$$

The total optical depth considered throughout was $T = 156$. Since the wings are optically thin, the photons escape in the wings freely and the emergent intensity is nearly the same as the incident intensity. The intensity profiles due to R_{III} and R_V are nearly the same. The source function is plotted as a function of frequency at various optical depths for a purely-scattering medium in Fig. 4. We see that the emergent source function differs from CRD by an order of magnitude in the wings for R_{II} and R_V. For a purely-scattering medium, there is a substantial contribution from radiation in the wings to the scattering integral. This contribution is enhanced by the fact that R_{II} and R_V are coherent in the wings. Thus the R_{II} and R_V emergent source functions are higher in the wings compared to CRD. R_{II} source function lies higher than R_V, since R_{II} is much more coherent in the wings as seen from Fig. 4(a). Similar result was also obtained by Heinzel (1983) for the case of optically-thin solar prominences.

Deeper in the medium, the radiation in the wings does not differ very much from the core. This is because the incident radiation has not undergone much of absorption in the core. Now we see that the differences between the source function values in the wings are reduced for R_{II}, R_V and CRD, and also that they do not deviate very much from the line centre. This can be seen from Fig. 4(b).

Further, we have considered an atmosphere with constant thermal sources ($\varepsilon = 10^{-3}$, $\beta = 0$, $B = 1$) and with no incident radiation. The source function corresponding to the functions R_{II}, R_{III} and R_V at various optical depths are shown in Fig. 5. Typical ratios are given in Table 1. The absorption in the wings is quite small and the bulk of the absorption takes place in the core. The partial coherency impedes the

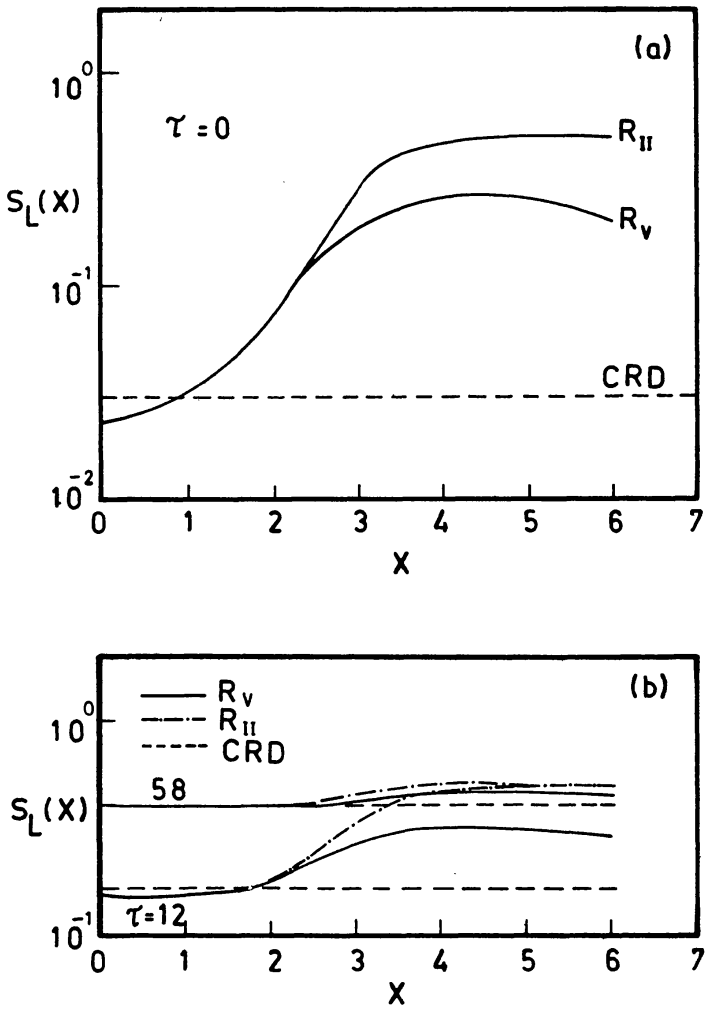

Figure 4. Source functions for R_{II}, R_V and CRD are compared for the case $\varepsilon = \beta = 0$; (a) $\tau = 0$, (b) $\tau = 12$ and 58.

Table 1. Ratios of emergent source functions at different frequencies.

x	$S_L(R_V)/S_L(R_{II})$	$S_L(R_V)/S_L(R_{III})$
0.38	0.99	1.02
1.89	0.98	1.03
3.89	1.80	0.72
5.97	8.18	0.68

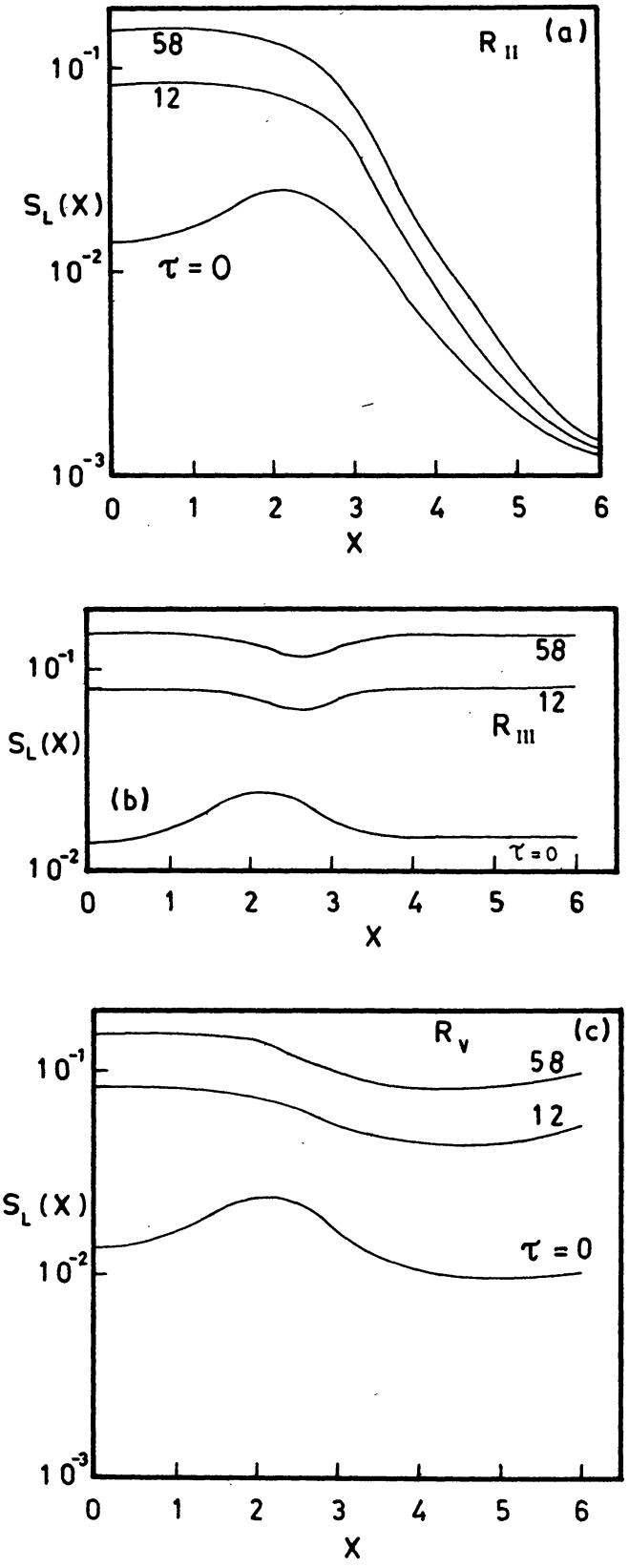

Figure 5. Source functions are plotted against x for the case $\varepsilon = 10^{-3}$, $\beta = 0$ for (a) R_{II} with $a_j = 2 \times 10^{-3}$, (b) R_{III} with $a_j = 2 \times 10^{-3}$, and (c) R_V with $a_i = a_j = 10^{-3}$.

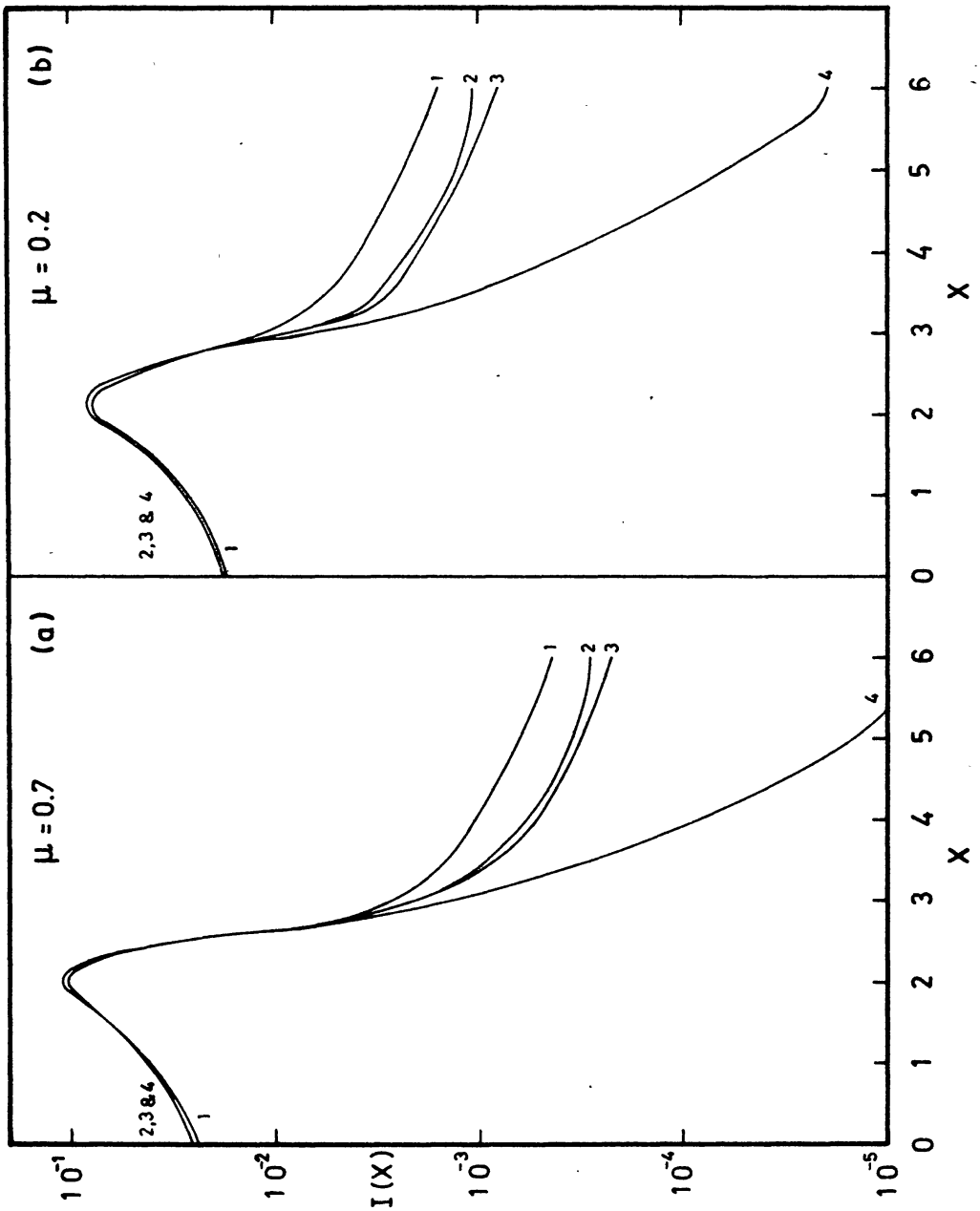

Figure 6. The emergent intensities for the case $\varepsilon = 10^{-3}$, $\beta = 0$ at (a) $\mu = 0.7$ and (b) $\mu = 0.2$. The numbers denote the following cases: (1) $R_{\rm III}$, $a_j = 2 \times 10^{-3}$; (2) $R_{\rm V}$, $a_i = a_j = 10^{-3}$; (3) $R_{\rm III}$, $a_j = 10^{-3}$; (4) $R_{\rm II}$, $a_j = 2 \times 10^{-3}$

escape of core photons through the wings. Therefore the efficiency of the transfer of photons to the wings depends on the noncoherency of the redistribution mechanism. R_{III}, being more noncoherent, transfers more photons to the wings.

This trend is very well exhibited by the source functions plotted. The result for R_{II} is in qualitative agreement with that of Hummer (1969) and for R_{III} with that of Vardavas (1976b).

The emergent intensity profiles for the above cases are plotted in Fig. 6. They reflect the behaviour of the source function. Similar emergent profiles have been obtained also by Hubený & Heinzel (1984), but for $T = 10^4$ and $\varepsilon = 10^{-4}$.

To see the effect of continuous absorption on line transfer with R_V redistribution, we considered a case with $\varepsilon = \beta = 10^{-3}$ and $S_C = B = 1$. We have plotted the frequency-dependent source function at various optical depths in Fig. 7(a). The source function

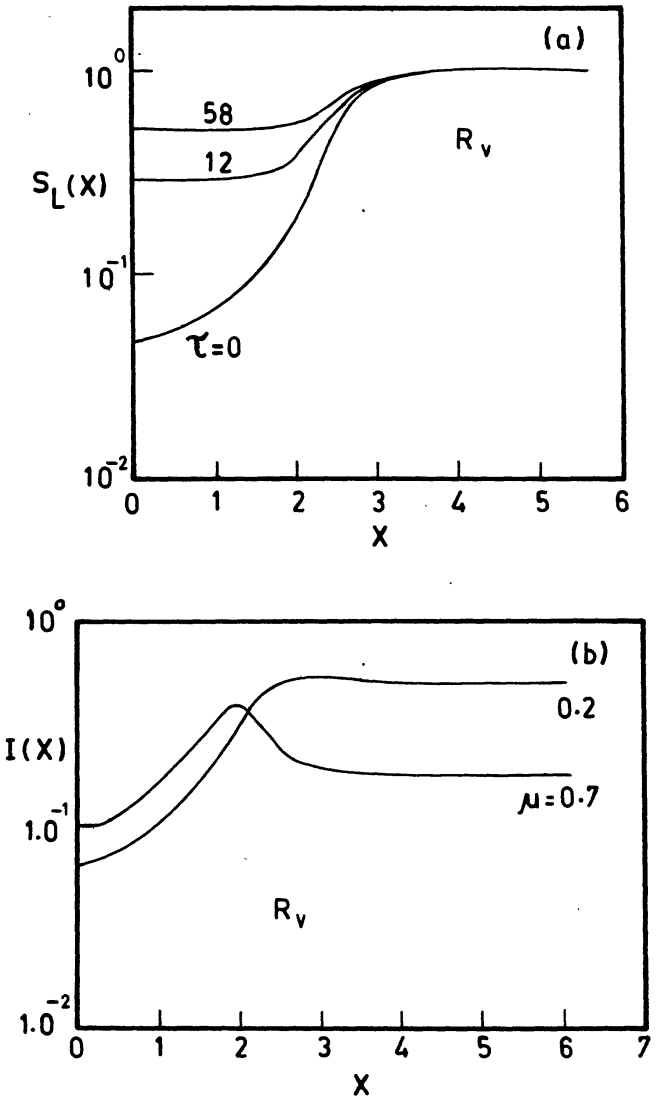

Figure 7. (a) Source function for $\tau = 0$, 12 and 58, and (b) emergent intensity at $\mu = 0.7$ and 0.2, for R_V with $\varepsilon = \beta = 10^{-3}$.

can be defined as

$$S(x) = \frac{1-\xi(x)}{\phi(x)} \int_{-\infty}^{\infty} R(x', x)\, J\,(x')\, dx' + \xi(x) B, \tag{12}$$

where

$$\xi(x) = \frac{\beta + \varepsilon\phi(x)}{\beta + \phi(x)}. \tag{13}$$

In the far wings $\xi(x) \simeq 1$ and therefore, $S(x) \to B$ at all optical depths. In the wings the intensity can be approximated by $I\,(x, \mu) \simeq B\beta T/\mu$. These characteristics are reflected in Fig. 7 both in the source functions as well as in the emergent intensity profiles. We see from the figure that in the wings, the line transfer is dominated by the overlying continuum.

5. Conclusions

For a purely scattering medium with frequency-independent incident radiation (white light), we find that $S_L(R_V)$ lies above $S_L(R_{III})$, since R_V is more coherent. For the same reason, $S_L(R_{II})$ lies above $S_L(R_V)$. For a medium with constant thermal sources and with no incident radiation, we find that the more noncoherent the redistribution, the higher is the source function in the wings. Emergent intensities just follow the source function variation. For the boundary conditions and the parameters considered, if we take $S_L(R_{II})$ and $S_L(R_{III})$ to correspond to two extreme situations, then $S_L(R_V)$ is in between these two, in qualitative agreement with the result of Hubený & Heinzel (1984). Furthermore, the wings are controlled by the overlying continuum for R_V redistribution when the continuous absorption is present.

The transition from plane-parallel situation to spherical symmetry is being studied by the present authors and the results will be presented in a separate paper.

Acknowledgement

We wish to thank Dr. P. Heinzel for his useful comments and suggestions.

References

Adams, T. F., Hummer, D. G., Rybicki, G. B. 1971, *J. quant. Spectrosc. radiat. Transfer*, **11**, 1365.
Finn, G. D. 1967, *Astrophys. J.*, **147**, 1085.
Grant, I. P., Peraiah, A. 1972, *Mon. Not. R. astr. Soc.*, **160**, 239.
Heinzel, P. 1981, *J. quant. Spectrosc. radiat. Transfer*, **25**, 483.
Heinzel, P. 1983, *Bull. astr. Inst. Csl.*, **34**, 7.
Heinzel, P., Hubený, I. 1982, *J. quant. Spectrosc. radiat. Transfer*, **27**, 1.
Heinzel. P., Hubený, I. 1983, *J. quant. Spectrosc. radiat. Transfer*, **30**, 77.
Hubený, I., Heinzel, P. 1984, *J. quant. Spectrosc. radiat. Transfer* (in press).
Hummer, D. G. 1962, *Mon. Not. R. astr. Soc.*, **125**, 21.

Hummer, D. G. 1969, *Mon. Not. R. astr. Soc.*, **145,** 95.
Matta, F., Reichel, A. 1971, *Math. Comput.*, **25,** 339.
Mihalas, D. 1978, *Stellar Atmospheres*, 2 Edn, Freeman, San Francisco.
Milkey, R. W., Mihalas, D. 1973, *Astrophys. J.*, **185,** 709.
Omont, A., Smith, E. W., Cooper, J. 1972, *Astr. J.*, **175,** 185.
Peraiah, A. 1978, *Kodaikanal Obs. Bull. Ser. A*, **2,** 115.
Vardavas, I. M. 1976a, *J. quant. Spectrosc. radiat. Transfer*, **16,** 1.
Vardavas, I. M. 1976b, *J. quant. Spectrosc. radiat. Transfer*, **16,** 715.
Vardavas, I. M. 1976c, *J. quant. Spectrosc. radiat. Transfer*, **16,** 781.